TECHNISCHE
UNIVERSITÄT
WIEN

BACHELOR THESIS

Stochastic Simulation of the Open Dicke Model

submitted by

Viktor Beck

for the degree of
Bachelor of Science

Supervisor:
Ass.-Prof. Dr. Peter Rabl

Co-supervisor:
Dipl.-Ing. Julian Huber

Atominstitut
Technische Universität Wien
Austria
April 13, 2021

Acknowledgements

First I would like to thank Professor Peter Rabl for supervising this bachelor thesis as well as Julian Huber for his patience regarding my endless amount of questions and his guidance on the field of quantum physics. Special thanks go to my parents Michaela and Markus and to my brother Nikolas for their everlasting support. As this thesis marks the end of my bachelor studies I would like to thank my physics high-school teacher Bernhard for introducing me to this subject. You were right - it wasn't that easy (but not that hard either).

Abstract

In case of the open Dicke model, simulations of the related master equations get ineffective for larger amounts of N two-level systems. It has been shown that in the Schwinger-Boson representation these master equations can be mapped onto sets of stochastic differential equations under certain approximations which is much more efficient to simulate in terms of computing power and necessary for larger amounts of two-level systems than solving directly the master equation.

The main goal of this thesis was therefore to write a set of programs to simulate two different systems - the quantum harmonic oscillator and a collective spin system - and then a combination of these to show how well this mapping and the further implications work.

As the stochastic equations for describing the systems of interest are not obvious, we start with the mathematical transformation of the master equation for the well-known quantum harmonic oscillator. Through so-called phase space distributions the master equation is mapped onto the desired form of a stochastic differential equation.

In the numerical part the exact and stochastic results of the featured systems are analysed and compared and we find that a spin system can indeed be well-approximated by the stochastic simulation of two bosonic modes. This implies an efficiency enhancement for computational calculation for the simulation of (large) spin systems.

Contents

1 Introduction

Light-matter interactions are the central topic of quantum optics. This aspect is studied here on the basis of the open Dicke model [1] which describes the coupling of N two-level systems to a common bosonic field mode and the system's exchange with its environment. A two-level system is the most simple form of a quantum system as its wavefunction can only oscillate between two possible, distinguishable states. Such a system is also called a qubit and forms the foundation for quantum computing.
The mathematical formulation of the Dicke model is expressed in terms of so-called master equations. They are given in the form of first order differential equations and usually describe the time evolution of the probabilities of a system whereby the *quantum* master equation is a generalized form, for it describes the time evolution of the system's density operator. These master equations can be simulated by numerical procedures like the Euler method [2] but for an increasing number of N two-level systems and therefore for an increasing dimension of the considered Hilbert space $d_{\mathcal{H}} = 2S + 1$ ($S = N/2$ is the spin quantum number) the simulation gets ineffective. This is a problem as one is often interested in systems containing large numbers of atoms or other particles. So instead of running a simulation for years we translate the master equation into a stochastic differential equation (SDE) which reduces the necessary computing power for simulating to a point where it is only dependent on the amount of time steps and different trajectories for the expectation values of interest.
Thus, the main goal of this thesis was to calculate the corresponding equations for two different models - the quantum harmonic oscillator and a spin system - and then a combination of these and, subsequently, to write a set of programs for each the exact and the stochastic approach. For that this thesis is separated into two parts: a theoretical part where the mapping onto the SDEs is specified and a numerical part - here the antecedent theoretical approaches come to their application via numerical procedures like the Euler or the Euler-Maruyama method [2].

The most valuable sources were the book *Quantum Optics* of D. F. Walls and G. J. Milburn [9] as well as the paper of J. Huber, P. Kirton and P. Rabl [5]. Also the the script of the latter - Professor Rabl - for his quantum optics class was very helpful. It conveys a great overview on the topic and should therefore be named here.

2 Theoretical framework

2.1 The master equation in Lindblad-form

The harmonic oscillator in quantum mechanics describes the behavior of a particle in a harmonic potential. It is a very important model for it is one of few systems in quantum-mechanics for which an exact analytical solution is known. The simplest form of the quantum harmonic oscillator is given by the von Neumann equation [7], an alternate form of the Schrödinger equation, which describes a closed system and reads

$$\frac{\partial \rho}{\partial t} = -\frac{i}{\hbar}[H, \rho]. \tag{2.1}$$

Here $H = \hbar\omega_0 a^\dagger a$ is the Hamiltonian of the system with the frequency ω_0 of the harmonic oscillator and the bosonic ladder operators a and $a^\dagger$. The density operator ρ provides a full description of a given quantum system and is defined by

$$\rho = \sum_{n,m} \rho_{nm} \left|n\right\rangle \left\langle m\right|, \quad \rho_{nn} \equiv p_n \leq 1. \tag{2.2}$$

If ρ contains only diagonal elements, $p_n \in \mathbb{R}$ is the probability to find the system in the state $|n\rangle$ (eigenbasis of ρ). Summing over p_n is therefore equal to $Tr[p_n] = 1$. Eq. (2.1) is called a master equation.

The system described above is now coupled to a thermal bath and a dissipation of the system is considered. Given these two adjustments, the (damped) quantum harmonic oscillator is now described by the master equation in Lindblad-form [5, 9]:

$$\begin{aligned} \frac{\partial \rho}{\partial t} = -i\omega_0[a^\dagger a, \rho] &+ \frac{\Gamma}{2}(N_{th}+1)(2a\rho a^\dagger - a^\dagger a\rho - \rho a^\dagger a) \\ &+ \frac{\Gamma}{2}N_{th}(2a^\dagger \rho a - aa^\dagger\rho - \rho aa^\dagger), \end{aligned} \tag{2.3}$$

which can also be written in a more compact form as

$$\frac{\partial \rho}{\partial t} = \mathcal{L}\rho = -\frac{i}{\hbar}[H, \rho] + \frac{\Gamma}{2}(N_{th}+1)\mathcal{D}[a]\rho + \frac{\Gamma}{2}N_{th}\mathcal{D}[a^\dagger]\rho, \tag{2.4}$$

where we have introduced the Lindblad superoperator

$$\mathcal{D}[c]\rho = 2c\rho c^\dagger - c^\dagger c\rho - \rho c^\dagger c. \tag{2.5}$$

Γ is the damping rate of the system and $N_{th} = (e^{\hbar\omega_0/k_BT} - 1)^{-1}$ is the thermal occupation number. The second term of Eq. (2.3) describes the loss of the system, the third term the gain.

For calculation of the expectation values we use the definition [9]:

$$\langle O(t)\rangle = Tr[O\rho(t)]. \tag{2.6}$$

Therefore,

$$\frac{d}{dt}\langle O(t)\rangle = Tr\left[O\frac{d\rho(t)}{dt}\right] = Tr\big[O\mathcal{L}(\rho(t))\big], \tag{2.7}$$

where O is an arbitrary operator. Here Eq. (2.6) is primarily used for numerically solving the expectation values, while Eq. (2.7) presents an analytical solution. For the given system we get

$$\frac{d}{dt}\langle a\rangle = -\big(i\omega_0 + \frac{\Gamma}{2}\big)\langle a\rangle, \tag{2.8}$$

$$\frac{d}{dt}\langle a^\dagger a\rangle = \Gamma\big(N_{th} - \langle a^\dagger a\rangle\big), \tag{2.9}$$

using the fact that the trace stays invariant for cyclic permutations. In time evolution the coupling to the bath causes the system to steadily equalize its temperature to the one of the bath, as can be seen in Eq. (2.9).

2.2 Coherent states

Coherent states [3] are states which come closest to describing the harmonic oscillator in classical physics as their expectation value of the electric field has the shape of a classical electromagnetic wave. They are not orthogonal and have minimal uncertainty ($\Delta x\Delta p = \frac{\hbar}{2}$). Another important property of a coherent state is that it is an eigenstate of the annihilation operator a with its eigenvalue $\alpha \in \mathbb{C}$:

$$a|\alpha\rangle = \alpha|\alpha\rangle \quad \text{as well as} \quad \langle\alpha| a^\dagger = \langle\alpha|\alpha^*. \tag{2.10}$$

Coherent states can also be described in the Fock space:

$$|\alpha\rangle = e^{-\frac{|\alpha|^2}{2}}\sum_{n=1}^{\infty}\frac{\alpha^n}{\sqrt{n!}}|n\rangle, \tag{2.11}$$

where

$$|n\rangle = \frac{(a^\dagger)^n}{\sqrt{n!}}|0\rangle. \tag{2.12}$$

This follows from the properties of the annihilation operator a and its adjoint, the creation operator $a^\dagger$, respectively:

$$a|n\rangle = \sqrt{n}\,|n-1\rangle, \quad a^\dagger|n\rangle = \sqrt{n+1}\,|n+1\rangle. \tag{2.13}$$

As stated above, they are non-orthogonal

$$\langle\beta|\alpha\rangle = e^{-\frac{1}{2}(|\beta|^2+|\alpha|^2-2\beta^*\alpha)} \neq \delta(\alpha-\beta) \tag{2.14}$$

and they fulfill the so-called completeness relation

$$\mathbb{1} = \frac{1}{\pi}\int d^2\alpha\,|\alpha\rangle\langle\alpha|\,. \tag{2.15}$$

The time evolution of a coherent state corresponds to a rotation around the zero point in the phase space, meaning that a coherent state remains a coherent state under time evolution:

$$|\alpha(t)\rangle = e^{-iHt/\hbar}\,|\alpha\rangle = |\alpha e^{-iE_n t/\hbar}\rangle\,. \tag{2.16}$$

The expectation value of $H = \hbar\omega a^\dagger a$ is the energy $E_n = \hbar\omega|\alpha|^2$. Therefore $|\alpha|^2$ can be interpreted as the mean photon number. The probability of measuring an occupation of n excitations is given by

$$P(\alpha) = |\,\langle n|\alpha\rangle\,|^2 = \frac{|\alpha|^{2n}}{n!}e^{-|\alpha|^2}, \tag{2.17}$$

which corresponds to a Poisson distribution.

2.3 Phase space distributions

For further calculations it is necessary to translate the density operator $\rho = \sum_{n,m}\rho_{n,m}\,|n\rangle\langle m|$ into different forms. These alternate representations of ρ are given by the P-, Q-, and Wigner function [9], which describe the system from a statistical point of view. Note that these functions deliver no regulary probability distributions as for some cases they can be negative or nonexistent - therefore, they are called quasi-probability functions.

The P-, Q-, and Wigner function describe different distributions in the phase space, depending on the considered state [9]:

- For a **Fock state** $\rho = |n\rangle\langle n|$:

$$P(\alpha) = \frac{1}{n!}\left(\frac{\partial^2}{\partial\alpha\partial\alpha^*}\right)^n\delta^2(\alpha), \tag{2.18}$$

$$Q(\alpha) = \frac{1}{\pi}e^{-|\alpha|^2}\frac{|\alpha|^{2n}}{n!}, \tag{2.19}$$

$$W(\alpha) = (-1)^n\frac{2}{\pi}e^{-2|\alpha|^2}L_n(4|\alpha|^2), \tag{2.20}$$

  with L_n denoting the n-th Laguerre polynomial.

- For a **coherent state** $\rho = |\alpha_0\rangle\langle\alpha_0|$:

$$P(\alpha) = \delta^2(\alpha-\alpha_0), \tag{2.21}$$

$$Q(\alpha) = \frac{1}{\pi} e^{-|\alpha-\alpha_0|^2}, \tag{2.22}$$

$$W(\alpha) = \frac{2}{\pi} e^{-2|\alpha-\alpha_0|^2}. \tag{2.23}$$

- For a **thermal state** $\rho = \frac{1}{Z} e^{-\frac{\hbar\omega}{k_B T} a^\dagger a}, \quad Z = (1 - e^{-\frac{\hbar\omega}{k_B T}})^{-1}$:

$$P(\alpha) = \frac{1}{\pi N_{th}} e^{-\frac{|\alpha|^2}{N_{th}}}, \tag{2.24}$$

$$Q(\alpha) = \frac{1}{\pi(N_{th}+1)} e^{-\frac{|\alpha|^2}{N_{th}+1}}, \tag{2.25}$$

$$W(\alpha) = \frac{1}{\pi(2N_{th}+1)} e^{-\frac{2|\alpha|^2}{2N_{th}+1}}. \tag{2.26}$$

As one can see, most of these functions, and especially the Q-function, describe a Gaussian distribution

$$f(x) = \frac{1}{\sqrt{2\pi\sigma^2}} e^{-\frac{(x-\mu)^2}{2\sigma^2}}, \tag{2.27}$$

where σ^2 is the variance and μ the expectation value of the random increment that determines the center of symmetry.

The P-, Q and Wigner function can be used to calculate expectation values of normally (P), anti-normally (Q), or symmetrically (W) ordered operators [9]:

$$\langle a^{\dagger m} a^n \rangle = \int d^2\alpha P(\alpha) \alpha^n \alpha^{*m}, \tag{2.28}$$

$$\langle a^m a^{\dagger n} \rangle = \int d^2\alpha Q(\alpha) \alpha^n \alpha^{*m}, \tag{2.29}$$

$$\langle a^{\dagger m} a^n \rangle_{Sym} = \int d^2\alpha W(\alpha) \alpha^n \alpha^{*m}. \tag{2.30}$$

In practice, this means that a different expectation value is obtained from each of these functions:

$$\langle a^\dagger a \rangle = \langle |\alpha|^2 \rangle_P, \quad \langle a a^\dagger \rangle = \langle |\alpha|^2 \rangle_Q, \quad \frac{1}{2} \langle a^\dagger a + a a^\dagger \rangle = \langle |\alpha|^2 \rangle_W. \tag{2.31}$$

Similarly,

$$\langle a^\dagger a^\dagger a a \rangle = \langle |\alpha|^4 \rangle_P, \tag{2.32}$$

$$\langle a^\dagger a^\dagger a a \rangle = \langle a a a^\dagger a^\dagger - 4 a a^\dagger + 2 \rangle = \langle |\alpha|^4 - 4|\alpha|^2 + 2 \rangle_Q, \tag{2.33}$$

$$\langle a^\dagger a^\dagger a a \rangle = \frac{1}{4} \langle a^\dagger a a^\dagger a + a^\dagger a a a^\dagger + a a^\dagger a^\dagger a + a a^\dagger a a^\dagger - a^\dagger a + a a^\dagger - 1 \rangle = \langle |\alpha|^4 - 2|\alpha|^2 - \frac{1}{4} \rangle_W, \tag{2.34}$$

which can be obtained by using the commutation relation $[a, a^\dagger] = 1$. For a sequence of the same operator like $\langle aa \rangle$ or just $\langle a \rangle$ they are of the same form for each of the functions

$$\langle a \rangle = \langle \alpha \rangle_{P|Q|W} \,. \tag{2.35}$$

However, the most important properties of the P-, Q- and Wigner function can be obtained by considering them in coherent states and by comparing these properties, the following general operator correspondences can be found [5, 9]:

$$a\rho \leftrightarrow \left(\alpha + \frac{(1-k)}{2}\frac{\partial}{\partial \alpha^*}\right) F(\alpha, t), \tag{2.36}$$

$$\rho a \leftrightarrow \left(\alpha - \frac{(1+k)}{2}\frac{\partial}{\partial \alpha^*}\right) F(\alpha, t), \tag{2.37}$$

$$a^\dagger \rho \leftrightarrow \left(\alpha^* - \frac{(1+k)}{2}\frac{\partial}{\partial \alpha}\right) F(\alpha, t), \tag{2.38}$$

$$\rho a^\dagger \leftrightarrow \left(\alpha^* + \frac{(1-k)}{2}\frac{\partial}{\partial \alpha}\right) F(\alpha, t). \tag{2.39}$$

The ladder operators are simply applied one after another onto ρ:

$$a^\dagger \rho a \leftrightarrow \left(\alpha^* - \frac{(1+k)}{2}\frac{\partial}{\partial \alpha}\right)\left(\alpha - \frac{(1+k)}{2}\frac{\partial}{\partial \alpha^*}\right) F(\alpha, t), \tag{2.40}$$

$$a^\dagger a \rho \leftrightarrow \left(\alpha^* - \frac{(1+k)}{2}\frac{\partial}{\partial \alpha}\right)\left(\alpha + \frac{(1-k)}{2}\frac{\partial}{\partial \alpha^*}\right) F(\alpha, t). \tag{2.41}$$

For $k = 1$, $F(\alpha, t) \equiv P(\alpha, t)$; for $k = -1$, $F(\alpha, t) \equiv Q(\alpha, t)$; for $k = 0$, $F(\alpha, t) \equiv W(\alpha, t)$. Consider that even though in Eq. (2.40) a is applied onto ρ from the right side, the operators on $F(\alpha, t)$ are always operating from the left side.
These correspondences can now be used to convert the master equation in Lindblad-form [9]

$$\begin{aligned}\frac{\partial \rho}{\partial t} = &-i\omega_0[a^\dagger a, \rho] + \frac{\Gamma}{2}(N_{th}+1)(2a\rho a^\dagger - a^\dagger a\rho - \rho a^\dagger a) \\ &+ \frac{\Gamma}{2}N_{th}(2a^\dagger \rho a - aa^\dagger \rho - \rho a a^\dagger),\end{aligned} \tag{2.42}$$

into the Fokker-Planck equation [9] for the quantum harmonic oscillator

$$\begin{aligned}\frac{\partial F(\alpha, t)}{\partial t} = &\left[\left(\frac{\Gamma}{2} + i\omega\right)\frac{\partial}{\partial \alpha}\alpha + \left(\frac{\Gamma}{2} - i\omega\right)\frac{\partial}{\partial \alpha^*}\alpha^*\right] F(\alpha, t) \\ &+ \Gamma\left(N_{th} + \frac{(1-k)}{2}\right)\frac{\partial^2}{\partial \alpha \partial \alpha^*} F(\alpha, t).\end{aligned} \tag{2.43}$$

2.4 The Fokker-Planck equation

The Fokker-Planck equation [9] is a partial differential equation that describes the time evolution of a probability density function $F(x,t)$ under the influence of drift, $A_j(x)$, and diffusion, $D_{ij}(x)$. It reads as follows:

$$\frac{\partial}{\partial t}F(x,t) = \left[-\frac{\partial}{\partial x_j}A_j(x) + \frac{1}{2}\sum_{i,j}\frac{\partial^2}{\partial x_i \partial x_j}D_{ij}(x)\right]F(x,t). \tag{2.44}$$

We name $D_{ij}(x)$ diffusion matrix because, in case of it being positive definite, it is broadening or diffusing $F(x,t)$, whereas $A_i(x)$ is responsible for the deterministic motion, which can be seen, by calculating the equations of motion for the expectation values:

$$\frac{d}{dt}\langle x_k\rangle = \langle A_k\rangle\,, \tag{2.45}$$

$$\frac{d}{dt}\langle x_k x_l\rangle = \langle x_k A_l\rangle + \langle x_l A_k\rangle + \frac{1}{2}\langle D_{kl} + D_{lk}\rangle\,. \tag{2.46}$$

For the quantum harmonic oscillator described by Eq. (2.44) they appear identical (as they should) to those calculated from the master equation in Lindblad-form (Eq. (2.8) and (2.9))

$$\frac{d}{dt}\langle a\rangle = -\big(i\omega_0 + \frac{\Gamma}{2}\big)\langle a\rangle\,, \tag{2.47}$$

$$\frac{d}{dt}\langle a^\dagger a\rangle = \Gamma\big(N_{th} - \langle a^\dagger a\rangle\big). \tag{2.48}$$

However, the Fokker-Planck equation is very laborious respectively time-consuming to solve and there are few special cases in which an exact analytical solution is possible. Therefore, it is crucial to translate the Fokker-Planck equation into a corresponding differential equation.

2.5 Stochastic differential equations

A stochastic differential equation (SDE) [2, 9] is a generalization of ordinary differential equations onto stochastic processes. The further implications of this generalization are covered in Itô calculus, named after its founder Itô Kiyoshi. A SDE is given by

$$dx(t) = a\big(x(t),t\big)dt + b\big(x(t),t\big)dW(t) \tag{2.49}$$

and can also be displayed in integral form

$$x(t) = x(t_0) + \int_{t_0}^{t} a\big(x(t'),t'\big)dt' + \int_{t_0}^{t} b\big(x(t'),t'\big)dW(t'). \tag{2.50}$$

This is called a Wiener process which is a normally distributed stochastic process with independent growth, described by the Wiener increment $dW(t) = W(t+\Delta t) - W(t)$. An

arbitrary function $f(x)$ in Itô calculus obeys Itô's Lemma:

$$df(x) = \frac{\partial f(x)}{\partial x}dx + \frac{1}{2}\frac{\partial^2 f(x)}{\partial x^2}dx^2. \tag{2.51}$$

This is because dW is proportional to $\sqrt{dt}$, therefore Itô differential equations have to be expanded up to second order. Next the time derivative of the expectation value of df is considered and $dx(t)$ is substituted from Eq. (2.49):

$$\begin{aligned}\frac{d}{dt}\big\langle f\big(x(t)\big)\big\rangle &= \frac{d}{dt}\bigg\langle \frac{\partial f(x)}{\partial x}\big[a\big(x(t),t\big)dt + b\big(x(t),t\big)dW(t)\big] \\ &\quad + \frac{1}{2}\frac{\partial^2 f(x)}{\partial x^2}\big[a\big(x(t),t\big)dt + b\big(x(t),t\big)dW(t)\big]^2\bigg\rangle \\ &= \bigg\langle a\big(x(t),t\big)\frac{\partial f(x)}{\partial x} + \frac{1}{2}b\big(x(t),t\big)^2\frac{\partial^2 f(x)}{\partial x^2}\bigg\rangle\end{aligned} \tag{2.52}$$

Note that $dW(t)$ disappears because of its expectation value being zero, whereas $dW(t)^2$ is proportional to dt and therefore does not. The term with dt^2 can also be neglected as it is too small. Since expectation values can be described using a probability distribution $P(x,t)$,

$$\big\langle g\big(x(t)\big)\big\rangle = \int g(x)P(x,t)dx \tag{2.53}$$

(for an arbitrary function $g(x)$) the equation from above can be rewritten as

$$\frac{d}{dt}\big\langle f\big(x(t)\big)\big\rangle = \int f(x)\frac{\partial P(x,t)}{\partial t}dx = \int \bigg[a(x,t)\frac{\partial f(x)}{\partial x} + \frac{1}{2}b(x,t)^2\frac{\partial^2 f(x)}{\partial x^2}\bigg]P(x,t)dx. \tag{2.54}$$

Integration by parts provides the following relation for disappearing boundary terms:

$$\int f(x)\frac{\partial P(x,t)}{\partial t}dx = \int f(x)dx\bigg[-\frac{\partial}{\partial x}a(x,t) + \frac{1}{2}\frac{\partial^2}{\partial x^2}b(x,t)^2\bigg]P(x,t). \tag{2.55}$$

Now it is easy to see that

$$\frac{\partial P(x,t)}{\partial t} = \bigg[-\frac{\partial}{\partial x}a(x,t) + \frac{1}{2}\frac{\partial^2}{\partial x^2}b(x,t)^2\bigg]P(x,t) \tag{2.56}$$

which is (again) the Fokker-Planck equation (2.44) with $a(x,t) \mathrel{\widehat{=}} A_j(x,t)$ and $b(x,t)^2 \mathrel{\widehat{=}} D_{ij}(x)$. As we now know that the coefficients from Eq. (2.49) correspond to the ones from Eq. (2.44), and therefore from Eq. (2.43), we can finally map the Fokker-Planck equation of the damped quantum harmonic oscillator onto a stochastic differential equation [9]:

$$d\alpha = -i\bigg(\omega - i\frac{\Gamma}{2}\bigg)\alpha dt + \sqrt{\frac{\Gamma}{2}(2N_{th}+1-k)}dW. \tag{2.57}$$

This works analogous for $d\alpha^*$ as it is the complex conjugate of this function. The diffusion matrix used for the mapping of Eq. (2.57) looks as follows:

$$D = \Gamma\left(N_{th} + \frac{(1-k)}{2}\right)\begin{pmatrix}1 & 0\\ 0 & 1\end{pmatrix}, \quad D = B^T B. \tag{2.58}$$

Note that the diagonal form of this matrix can be obtained by changing ∂x_j to ∂x_j^* in the second-order derivative in the definition of the Fokker-Planck equation (2.44). The advantage of this mapping is that a full calculation of the probability distributions is no longer necessary - instead, the expectation values can be evaluated by averaging over a large number of these stochastic trajectories.

2.6 Superradiant decay

The spin [7] in general is often interpreted as the intrinsic angular momentum of an elementary particle as it follows the conservation of momentum and stays invariant for geometric transformation. This analogy works only for some of the calculations - for example, if the orbital and the intrinsic angular momentum are taken into account, an electron 'circling' around a nucleus would have multiple times the speed of light. The spin is also co-responsible (with the angular momentum) for the magnetic moment of a particle.

Here we consider collective spin systems, which represent, for example, a collection of N two-level systems. The properties of a collective spin are described by its operators

$$S^2 \left|s, m_s\right\rangle = \hbar^2 s(s+1) \left|s, m_s\right\rangle, \quad S_z \left|s, m_s\right\rangle = \hbar m_s \left|s, m_s\right\rangle \tag{2.59}$$

and the ladder operators

$$S_\pm \left|s, m_s\right\rangle = \sqrt{s(s+1) - m_s(m_s \pm 1)} \left|s, m_s \pm 1\right\rangle, \quad S_\pm = (S_x \pm i S_y) \tag{2.60}$$

for the spin quantum numbers s and $m_s = \{-s, -s+1, ..., s-1, s\}$. s can be integer (bosons) or half-integer (fermions). Also important are the commutation relations between these operators:

$$[S_i^z, S_j^\pm] = \delta_{ij} S_j^\pm, \quad [S_i^+, S_j^-] = 2\delta_{ij} S_j^z. \tag{2.61}$$

As the dimension of their Hilbert Space $d_\mathcal{H} = 2^N$ grows exponentially it is hardly possible to simulate large ensembles of two-level systems - therefore, they are modeled as a single collective spin which reduces the Hilbert space to $d_\mathcal{H} = 2S+1$. Like the harmonic oscillator, such a spin system can then be described by the master equations of the Dicke model [1] - a single mode coupled to N two-level systems. This is shown in the following section for a superradiant decay [4] which can occur in collective spin systems.

2.6.1 Master equation

The previous steps from the master equation to a SDE for the quantum harmonic oscillator can be done equivalently for the spin system. The master equation of a superradiant decay [4, 5] is given by

$$\frac{d\rho(t)}{dt} = \frac{\Gamma}{2}\mathcal{D}[S_-]\rho, \tag{2.62}$$

where the dissipation of the system is identified as spontaneous emission. The spin operators can be expressed alternatively by bosonic ladder operators using the Schwinger boson representation [8]:

$$S_+ = a^\dagger b, \quad S_- = ab^\dagger \quad \text{and} \quad S_z = \frac{1}{2}(a^\dagger a - b^\dagger b). \tag{2.63}$$

Note that $[a, b] = 0$ as they operate in different spaces. The usual commutation relations for the spin as given in Eq. (2.61) also stay preserved.

2.6.2 Fokker-Planck equation

Equation (2.62) in bosonic ladder operators,

$$\frac{d\rho(t)}{dt} = \frac{\Gamma}{2}\big(2ab^\dagger\rho a^\dagger b - a^\dagger b a b^\dagger\rho - \rho a^\dagger b a b^\dagger\big), \tag{2.64}$$

can be translated into the Fokker-Planck equation [9] using the operator correspondences (2.36) to (2.39) for the phase space distributions. While calculating, the truncated Wigner approximation [6] is used where derivatives of third or higher orders are discarded because they impede efficient stochastic simulation. For spin systems this approximation gets accurate for large S [5]. We get

$$\begin{aligned}\frac{dF(\alpha,\beta,t)}{dt} = \frac{\Gamma}{2}\Bigg[&\frac{\partial}{\partial\alpha}\left(|\beta|^2 + \frac{(1+k)}{2}\right)\alpha - \frac{\partial}{\partial\beta}\left(|\alpha|^2 - \frac{(1-k)}{2}\right)\beta + \frac{\partial}{\partial\alpha^*}\left(|\beta|^2 + \frac{(1+k)}{2}\right)\alpha^* \\ &- \frac{\partial}{\partial\beta^*}\left(|\alpha|^2 - \frac{(1-k)}{2}\right)\beta^* + (1-k)\frac{\partial^2}{\partial\alpha\partial\alpha^*}\left(|\beta|^2 + \frac{(1+k)}{2}\right) \\ &+ (1+k)\frac{\partial^2}{\partial\beta\partial\beta^*}\left(|\alpha|^2 - \frac{(1-k)}{2}\right) - \frac{\partial^2}{\partial\alpha\partial\beta}\alpha\beta - \frac{\partial^2}{\partial\alpha^*\partial\beta^*}\alpha^*\beta^*\Bigg]F(\alpha,\beta,t).\end{aligned} \tag{2.65}$$

One can see that every term has a complex conjugated double - consequently, the second-order derivatives are multiplied by a factor 2 as they are invariant for complex conjugating.

By looking at the diffusion matrix ($x_1 \equiv \alpha$, $x_2 \equiv \alpha^*$, $x_3 \equiv \beta$, $x_4 \equiv \beta^*$)

$$D = \frac{\Gamma}{2}\begin{pmatrix} \frac{(1-k)}{2}\left(|\beta|^2 + \frac{(1+k)}{2}\right) & 0 & 0 & -\alpha\beta \\ 0 & \frac{(1-k)}{2}\left(|\beta|^2 + \frac{(1+k)}{2}\right) & -\alpha^*\beta^* & 0 \\ 0 & -\alpha\beta & \frac{(1+k)}{2}\left(|\alpha|^2 - \frac{(1-k)}{2}\right) & 0 \\ -\alpha^*\beta^* & 0 & 0 & \frac{(1+k)}{2}\left(|\alpha|^2 - \frac{(1-k)}{2}\right) \end{pmatrix} \tag{2.66}$$

we find that it is not positive definite, which would be necessary for $D = B^T B$. A so-called positive diffusion approximation [5] is therefore performed, which allows us to neglect the terms containing $\frac{\partial^2}{\partial\alpha\partial\beta}$ or its complex conjugate as they prevent the positivity of the matrix and do not change the solutions decisively. Therefore, the anti-diagonal elements of D are set to 0, leaving behind the practical form of a diagonal matrix which makes further calculation from D to B obsolete ($B = \sqrt{D}$, $B = B^T$).

2.6.3 Stochastic differential equations

As the diffusion matrix D is now known the equation from above can be mapped onto stochastic differential equations:

$$d\alpha(t) = -\frac{\Gamma}{2}\left(|\beta|^2 + \frac{(1+k)}{2}\right)\alpha dt + \sqrt{\frac{\Gamma(1-k)}{4}\left(|\beta|^2 + \frac{1+k}{2}\right)}dW, \tag{2.67}$$

$$d\beta(t) = \frac{\Gamma}{2}\left(|\alpha|^2 - \frac{(1-k)}{2}\right)\beta dt + \sqrt{\frac{\Gamma(1+k)}{4}\left(|\alpha|^2 - \frac{1-k}{2}\right)}dW \tag{2.68}$$

and their complex conjugates. Note that $dW \in \mathbb{C}$ and therefore, $dW = dW_1 + idW_2$. With these equations it is now possible to simulate the expectation values for the various spin operators stochastically.

2.7 Spin system coupled to the harmonic oscillator

In this section a 'new' system is described as a combination of the previously covered models of the quantum harmonic oscillator and the spin system. This can be understood as a lossy cavity in the form of a dissipative spin system coupled to a quantum harmonic oscillator.

2.7.1 Master equation

The master equation for the system is given by

$$\frac{d\rho}{dt} = -i[H,\rho] + \frac{\Gamma}{2S}\mathcal{D}[S_-]\rho + \kappa\mathcal{D}[c]\rho \tag{2.69}$$

and the Hamiltonian is

$$H = \frac{g}{\sqrt{2S}}\big(S_+c + S_-c^\dagger\big), \tag{2.70}$$

which describes the coupling between the spin system and the harmonic oscillator. Γ is the dissipation in the form of spontaneous emission and κ is the damping rate of the harmonic oscillator.

The whole master equation expressed in bosonic ladder operators using the Schwinger-Boson representation [8] reads

$$\begin{aligned}\frac{d\rho}{dt} =& -i\frac{g}{\sqrt{2S}}\big(a^\dagger bc\rho + ab^\dagger c^\dagger\rho - \rho a^\dagger bc - \rho ab^\dagger c^\dagger\big) \\ &+ \frac{\Gamma}{2S}\big(2ab^\dagger\rho a^\dagger b - a^\dagger bab^\dagger\rho - \rho a^\dagger bab^\dagger\big) + \kappa\big(2c\rho c^\dagger - c^\dagger c\rho - \rho c^\dagger c\big),\end{aligned} \tag{2.71}$$

from which the expectation values were calculated using

$$\frac{d}{dt}\langle O(t)\rangle = Tr\big[O\mathcal{L}(\rho(t))\big] \tag{2.72}$$

and the commutation relations for ladder operators like $[a, a^\dagger] = 1$:

$$\frac{d}{dt}\langle c\rangle = -i\frac{g}{\sqrt{2S}}\langle S_-\rangle - \kappa\langle c\rangle, \tag{2.73}$$

$$\frac{d}{dt}\langle S_-\rangle = 2i\frac{g}{\sqrt{2S}}\langle S_z c\rangle + 2\frac{\Gamma}{2S}\langle S_z S_-\rangle, \tag{2.74}$$

$$\frac{d}{dt}\langle S_x\rangle = i\frac{g}{\sqrt{2S}}\langle S_z(c - c^\dagger)\rangle + \frac{\Gamma}{2S}\langle S_z(S_+ + S_-)\rangle, \tag{2.75}$$

$$\frac{d}{dt}\langle S_y\rangle = -\frac{g}{\sqrt{2S}}\langle S_z(c + c^\dagger)\rangle - i\frac{\Gamma}{2S}\langle S_z(S_+ - S_-)\rangle, \tag{2.76}$$

$$\frac{d}{dt}\langle S_z\rangle = -i\frac{g}{\sqrt{2S}}\langle S_+c - S_-c^\dagger\rangle - \frac{\Gamma}{2S}\langle S_-S_+ + S_z\rangle. \tag{2.77}$$

We consider two cases:

1. $g = \kappa = 0$, $\Gamma \neq 0$: This is practically the collective spin system from Section 2.

2. $g = 1$, $\kappa > g$, $\Gamma = 0$: Here the bare dissipation of the spin system vanishes, though the Hamiltonian of the interaction is still present - consequently, the dissipation of the spin system is (or can be) caused indirectly by the harmonic oscillator. For $\kappa \gg g$ Eq. (2.73) can be set to 0 for it converges much faster to 0 than the other expectation values - consequently,
$$\langle c\rangle \approx -i\frac{g}{\sqrt{2S}\kappa}\langle S_-\rangle. \tag{2.78}$$

Furthermore, we approximate $\langle S_z c\rangle \approx \langle S_z\rangle \cdot \langle c\rangle$ which allows us to insert the relation above into Eq. (2.73) to (2.77) and we get

$$\frac{d}{dt}\langle S_-\rangle = \frac{g^2}{S\kappa}\langle S_z S_-\rangle\,, \tag{2.79}$$

$$\frac{d}{dt}\langle S_x\rangle = \frac{g^2}{2S\kappa}\langle S_z(S_+ + S_-)\rangle\,, \tag{2.80}$$

$$\frac{d}{dt}\langle S_y\rangle = -i\frac{g^2}{2S\kappa}\langle S_z(S_+ - S_-)\rangle\,, \tag{2.81}$$

$$\frac{d}{dt}\langle S_z\rangle = -\frac{g^2}{S\kappa}\langle S_- S_+ + S_z\rangle\,. \tag{2.82}$$

By comparing the expectation values of both cases we find that they are of the same form for

$$\Gamma = \frac{g^2}{\kappa} \tag{2.83}$$

which legitimises the approximation. Further examination of this aspect is covered in the numerical part.

2.7.2 Fokker-Planck equation

The Fokker-Planck equations [9] for each term separately were calculated as follows using the usual correspondences from Eq. (2.36) to (2.39):

$$-i[H,\rho] \mathrel{\widehat{=}} i\frac{g}{\sqrt{2S}}\left[\frac{\partial}{\partial\alpha}\beta\gamma + \frac{\partial}{\partial\beta}\alpha\gamma^* + \frac{\partial}{\partial\gamma}\alpha\beta^* + c.c.\right]F(\alpha,\beta,\gamma,t) \tag{2.84}$$

where the derivatives of second- or higher-order were neglected under the truncated Wigner approximation [6] for they impede efficient simulation and do not affect the process considerably;

$$\begin{aligned}\frac{\Gamma}{2S}\mathcal{D}[S_-]\rho \mathrel{\widehat{=}} \frac{\Gamma}{2S}\Bigg[&\frac{\partial}{\partial\alpha}\left(|\beta|^2 + \frac{(1+k)}{2}\right)\alpha - \frac{\partial}{\partial\beta}\left(|\alpha|^2 - \frac{(1-k)}{2}\right)\beta - \frac{\partial^2}{\partial\alpha\partial\beta}\alpha\beta \\ &+ \frac{(1-k)}{2}\frac{\partial^2}{\partial\alpha\partial\alpha^*}\left(|\beta|^2 + \frac{(1+k)}{2}\right) + \frac{(1+k)}{2}\frac{\partial^2}{\partial\beta\partial\beta^*}\left(|\alpha|^2 - \frac{(1-k)}{2}\right) + c.c.\Bigg]F(\alpha,\beta,\gamma,t)\end{aligned} \tag{2.85}$$

- here the truncated Wigner approximation is performed again, neglecting derivatives of third- or higher-order;

$$\kappa\mathcal{D}[c]\rho \mathrel{\widehat{=}} \kappa\left[\frac{\partial}{\partial\gamma}\gamma + \frac{(1-k)}{2}\frac{\partial^2}{\partial\gamma\partial\gamma^*} + c.c.\right]F(\alpha,\beta,\gamma,t); \tag{2.86}$$

c.c. means 'complex conjugated', so every term in the respective bracket has an additional complex conjugated double.

2.7.3 Stochastic differential equations

The Fokker-Planck equations [9] can then again be implemented as diffusion matrix which is practically the one from Eq. (2.66) from the spin system with an expansion to a 6×6 matrix for $x_5 \equiv \gamma$ and $x_6 \equiv \gamma^*$. The new entries for the second-order derivatives regarding γ and γ^* are positive and therefore do not disturb the positivity of the matrix. So the positive diffusion approximation [5] refers to the same entries as in Eq. (2.66), leaving a diagonal matrix where $B = \sqrt{D}$. The new subsystem[1] is

$$D_{\gamma\gamma^*} = \kappa \begin{pmatrix} \frac{(1-k)}{2} & 0 \\ 0 & \frac{(1-k)}{2} \end{pmatrix}. \tag{2.87}$$

The Fokker-Planck equation [9] mapped onto SDEs is therefore:

$$d\alpha(t) = -\left[\frac{\Gamma}{2S}\left(|\beta|^2 + \frac{(1+k)}{2}\right)\alpha + i\frac{g}{\sqrt{2S}}\beta\gamma\right]dt + \sqrt{\frac{\Gamma(1-k)}{4S}\left(|\beta|^2 + \frac{1+k}{2}\right)}dW, \tag{2.88}$$

$$d\beta(t) = \left[\frac{\Gamma}{2S}\left(|\alpha|^2 - \frac{(1-k)}{2}\right)\beta - i\frac{g}{\sqrt{2S}}\alpha\gamma^*\right]dt + \sqrt{\frac{\Gamma(1+k)}{4S}\left(|\alpha|^2 - \frac{1-k}{2}\right)}dW, \tag{2.89}$$

$$d\gamma(t) = -\left(\kappa\gamma + i\frac{g}{\sqrt{2S}}\alpha\beta^*\right)dt + \sqrt{\frac{\kappa(1-k)}{2}}dW. \tag{2.90}$$

[1] The whole Matrix D is too big to fit the page.

3 Numerical implementation and results

In this chapter the previous theoretical deliberations will be applied to computational procedures using the Euler or the Euler-Maruyama method [2] for solving the given differential equations. These code scripts were written with Python 3.

3.1 Numerical tools

3.1.1 Euler method

The Euler method [2] is a simple numerical procedure for solving first order ordinary differential equations. The initial value problem is given by:

$$\dot{y}(t) = f(t, y), \quad y(t_0) = y_0, \tag{3.1}$$

for an arbitrary $f(y, t)$. Next, a step size Δt, which is small enough to preserve the characteristics of the function $f(t, y)$, is to be chosen. The importance of a small Δt can be seen in the following relation which describes a numerical procedure for the time evolution of y:

$$y_{n+1} = y_n + \Delta t f(t_n, y_n) \tag{3.2}$$

with

$$t_n = t_0 + n\Delta t, \quad n = 0, 1, 2, ... \tag{3.3}$$

Equation (3.2) provides an approximation for $y(t)$ with an entry for each time step t_n. The smaller Δt is, the more accurate the approximation gets. Note that the initial condition y can be a vector or a matrix. The local error is proportional to n^2. In code the Euler method (for Eq. (2.3)) was written like this:

```
import numpy as np

def euler(func,rho0,t,step):
    Y=np.zeros((len(t),dim))
    y=rho0
    for i in range(0,len(t)-1):
        for j in range(0,dim):
            Y[i,j]=y[j,j]
        y=y+step*func(y,a,a_dag)
    return Y
```

3.1.2 Euler-Maruyama method

Based on the Euler method the Euler-Maruyama method [2], or stochastic Euler method, works for stochastic ordinary differential equations such as

$$dy(t) = a(t, y)dt + b(t, y)dW. \tag{3.4}$$

The approximation of $y(t)$ is calculated as follows:

$$y_{n+1} = y_n + a(t, y)\Delta t + b(t, y)\Delta W_n. \tag{3.5}$$

$\Delta W_n = W_{n+1} - W_n$ is the random increment which describes a certain randomness of the system in the manner of Brownian motion (expectation value 0, variance Δt)

$$\Delta W = \sqrt{\Delta t} x_i, \quad x_i \in N(0, 1). \tag{3.6}$$

x_i is a random number from a normalized Gaussian distribution $N(0, 1)$. The Euler-Maruyama method (for Eq. (2.57)) was programmed as follows:

```
import numpy as np

def dW(step):
    sqrtdt=np.sqrt(step)
    dW_real=np.random.normal(0.0,sqrtdt,size=(1,m))
    dW_imaginary=1j*np.random.normal(0.0,sqrtdt,size=(1,m))
    return (dW_real+dW_imaginary)

def maruyama(a,b,t,step,dW):
    y=np.ones((len(t),m),dtype=complex) #for P-function
    for i in range(0,len(t)-1):
        y[i+1]=y[i]+a*step*y[i]+b*dW(step)
    return y
```

Note that `np.normal(size=(1,m))` creates a vector of `m` normal distributed numbers for the `m` different trajectories (`m` $= n_{traj}$).

3.2 Harmonic oscillator

3.2.1 Master equation

At first the quantum harmonic oscillator in Lindblad-form [9] is considered:

$$\begin{aligned}\frac{\partial \rho}{\partial t} = -i\omega[a^\dagger a, \rho] + \frac{\Gamma}{2}(N_{th} + 1)(2a\rho a^\dagger - a^\dagger a\rho - \rho a^\dagger a) \\ + \frac{\Gamma}{2} N_{th}(2a^\dagger \rho a - aa^\dagger \rho - \rho aa^\dagger).\end{aligned} \tag{3.7}$$

For an analysis of the exact system dynamics it is practical to visualize $\rho(t)$. Therefore, a simple program was written, using the Euler method for calculating the differential equation given by Eq. (3.7). As we are only interested in the populations p_n, it is sufficient to only evolve the diagonal elements of ρ in time - this way, a lot of computing power is spared which is important because $\rho(t)$ is programmed as a three-dimensional $n \times n \times n_t$ matrix where n_t indicates the amount of time-steps Δt. n is the amount of included number states of our truncated Hilbert space and consequently determines the dimension of the matrices respectively the operators we use for numerically solving the master equation. Therefore, the simulation of the system dynamics works well for rather small n.

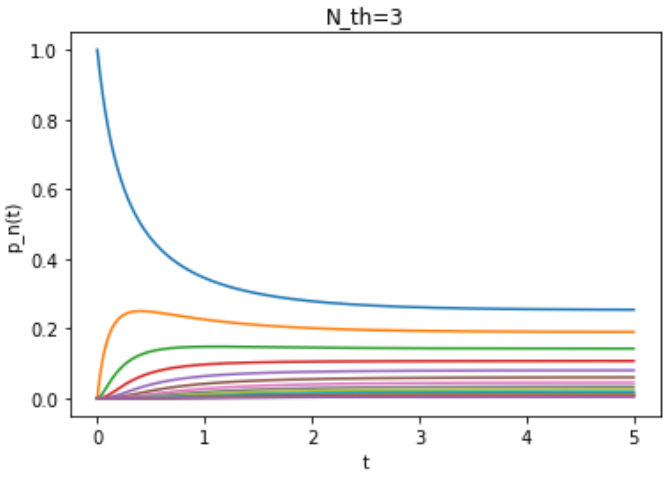

Figure 3.1: Time evolution of the diagonal elements $p_n(t)$ of $\rho(t)$, starting with a fully occupied ground state ($p_1(t=0)=1$); $N_{th}=3$, $n=[0;15]$

The annihilation operator a and the creation operator $a^\dagger$ were constructed like this:

$$a = \begin{pmatrix} 0 & \sqrt{1} & & & \\ & 0 & \sqrt{2} & & \\ & & 0 & \sqrt{3} & \\ & & & 0 & \ddots \\ & & & & \ddots \end{pmatrix}, \quad a^\dagger = \begin{pmatrix} 0 & & & & \\ \sqrt{1} & 0 & & & \\ & \sqrt{2} & 0 & & \\ & & \sqrt{3} & 0 & \\ & & & \ddots & \ddots \end{pmatrix}. \tag{3.8}$$

The dimension of these $n \times n$ matrices depends on the number of states n respectively the mean photon number in case of coherent states. 'Usually' their dimension would be infinite but for plausible reasons a truncated Hilbert space is considered.

As it is not always clear how many number states n are necessary for an adequate representation of the system dynamics, it is practical to write a program that visualizes the alteration of $p_n(t)$ regarding n in the steady state (in Fig. 3.1 it would be at about $t=4$). One can see in Figure 3.2, for small changes of the value of the thermal occupation number N_{th}, the necessary amount of states n can get relatively high which means that a lot of

computing power is needed. If not enough states are considered, the numerical solution will differ from the analytical solution and worsen the approximation.

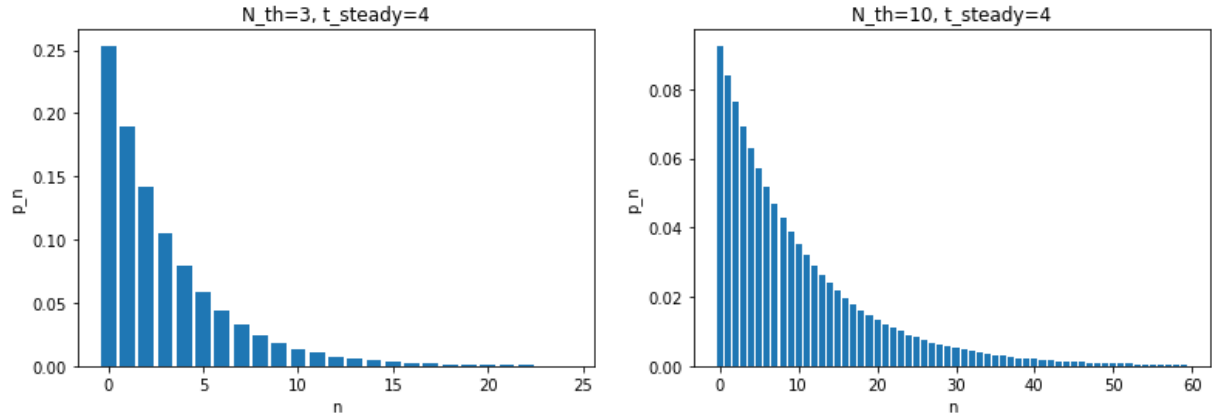

Figure 3.2: $p_n(t = 4)$ regarding n for $N_{th} = \{3; 10\}$; the sufficient value for the dimension of the Hilbert space is $\sim 10N_{th}$.

The following definition was used for the calculation of the expectation values:

$$\langle O(t) \rangle = Tr[O\rho(t)] \tag{3.9}$$

for an arbitrary operator $O(t)$. For $\langle a^\dagger a \rangle (t)$ this is equivalent to the analytical solution of

$$\frac{d}{dt} \langle a^\dagger a \rangle = \Gamma \big(N_{th} - \langle a^\dagger a \rangle \big), \tag{3.10}$$

which is

$$\langle a^\dagger a \rangle (t) = e^{-\Gamma t} \big(\langle a^\dagger a \rangle (0) - N_{th} \big) + N_{th}. \tag{3.11}$$

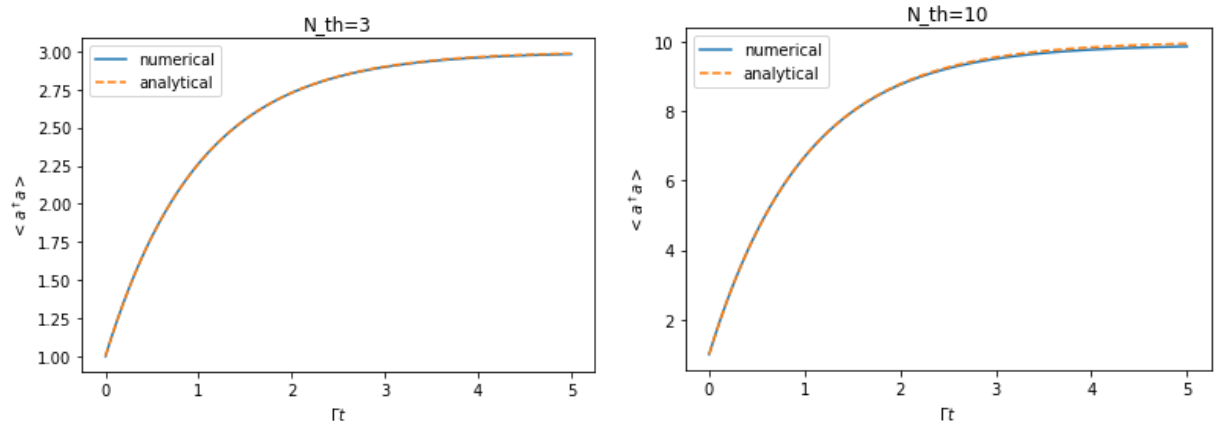

Figure 3.3: $\langle a^\dagger a\rangle(t)$ for $N_{th} = \{3; 10\}$; note that the (very) small difference between the analytical and the numerical solution for $N_{th} = 10$ occurs because n was chosen slightly too small ($n = 70$) - as explained above.

3.2.2 Stochastic differential equations

The implementations of the previous section are now considered in the equivalent stochastic differential equation

$$d\alpha = -i\left(\omega - i\frac{\Gamma}{2}\right)\alpha dt + \sqrt{\frac{\Gamma}{2}(2N_{th} + 1 - k)}dW. \tag{3.12}$$

The P-, Q- and Wigner function demand different initial values, depending on the form of the respective function and therefore, on the considered state (Eq. (2.18) to (2.25)). For coherent states:

$$P(\alpha) = \delta^2(\alpha - \alpha_0), \quad Q(\alpha) = \frac{1}{\pi}e^{-|\alpha-\alpha_0|^2}, \quad W(\alpha) = \frac{2}{\pi}e^{-2|\alpha-\alpha_0|^2}. \tag{3.13}$$

Consequently, the starting values for the P-representation have to be set to 1. For calculation in the Q- and Wigner-representation we initialize the matrix with normally distributed random numbers and standard deviations $\sigma_Q = \frac{1}{\sqrt{2}}$ and $\sigma_W = \frac{1}{2}$. The corrections of the expectation values also have to be taken into account as they look different for each of the three functions for

$$\langle a^\dagger a\rangle = \langle|\alpha|^2\rangle_P = \langle|\alpha|^2 - 1\rangle_Q = \langle|\alpha|^2 - \frac{1}{2}\rangle_W, \tag{3.14}$$

$$\langle a^\dagger a^\dagger aa\rangle = \langle|\alpha|^4\rangle_P = \langle|\alpha^4| - 4|\alpha|^2 + 2\rangle_Q = \langle|\alpha|^4 - 2|\alpha|^2 - \frac{1}{4}\rangle_W. \tag{3.15}$$

A calculation of the same initial conditions, while considering the appropriate adjustments, will deliver the same results for all the three functions.

Further examination or verification of the results can be done by calculating the second-order correlation function [9]

$$g^{(2)}(0) = \frac{\langle c^\dagger c^\dagger cc \rangle}{\langle c^\dagger c \rangle^2} = \frac{\langle n^2 \rangle - \langle n \rangle}{\langle n \rangle^2} = \frac{(\Delta n)^2 - \langle n \rangle}{\langle n \rangle^2}, \tag{3.16}$$

which gives a certain value, depending on the state of the system, or more precisely the variance of the respective state:

- Fock state: $(\Delta n)^2 = 0 \quad \Rightarrow g^{(2)}(0) = 1 - \frac{1}{n} \quad \text{for} \quad n \geq 1$
- coherent state: $(\Delta n)^2 = \langle n \rangle \quad \Rightarrow g^{(2)}(0) = 1$
- thermal state: $(\Delta n)^2 = \langle n^2 \rangle + \langle n \rangle \quad \Rightarrow g^{(2)}(0) = 2$

The following plots were initialized with the initial conditions for coherent states (see above):

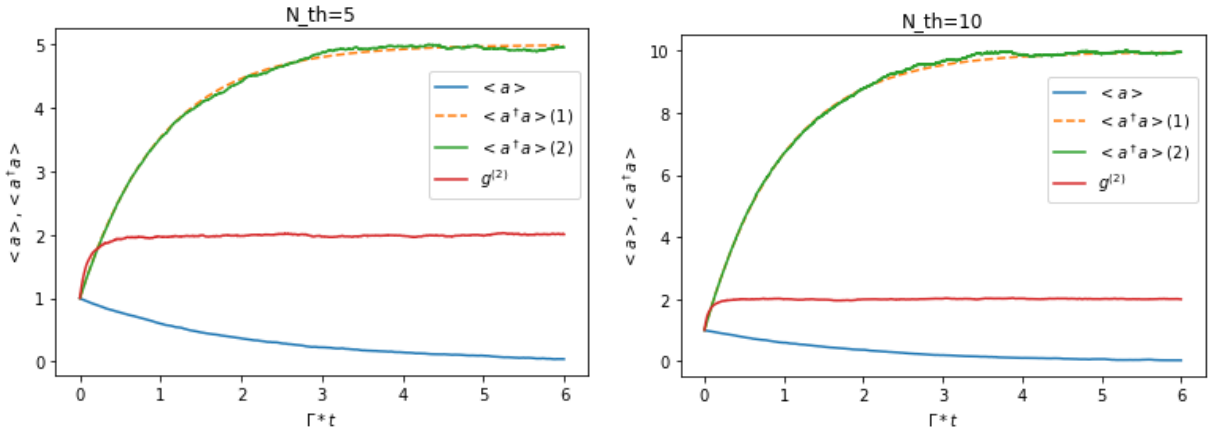

Figure 3.4: $\langle a \rangle (t)$, $\langle a^\dagger a \rangle (t)$ exact (1) and stochastic (2), and $g^{(2)}$ for $N_{th} = \{5; 10\}$ using the P-function; the expectation values were calculated by averaging over $n_{traj} = 15000$ trajectories.

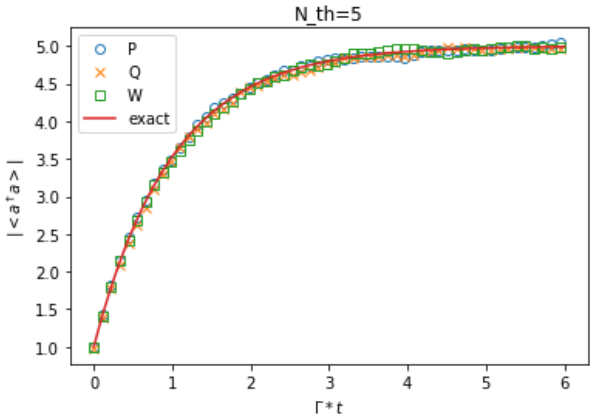

Figure 3.5: $\langle a^\dagger a \rangle (t)$ for $N_{th} = 5$ using the P-, Q- and Wigner function; $n_{traj} = 15000$ for the stochastic plot markers; one can see that the three functions differ slightly even for a large amount of trajectories - this is because of the stochastic nature of the simulation and could be improved by an even larger amount of trajectories.

3.3 Superradiant decay

3.3.1 Master equation

The exact solution for the system is given by the master equation

$$\frac{d\rho(t)}{dt} = \frac{\Gamma}{2}\big(2S_-\rho S_+ - S_+S_-\rho - \rho S_+S_-\big). \tag{3.17}$$

The ladder operators S_+ and S_- were constructed using the following definition [7]:

$$S_\pm \left|s, m_s\right\rangle = \sqrt{s(s+1) - m_s(m_s \pm 1)}\left|s, m_s \pm 1\right\rangle, \quad m_s = \{s, s-1, ..., 1-s, -s\}. \tag{3.18}$$

In matrix form we get, for example, for $s = 2$

$$S_+ = \begin{pmatrix} 0 & 2 & 0 & 0 & 0 \\ 0 & 0 & \sqrt{6} & 0 & 0 \\ 0 & 0 & 0 & \sqrt{6} & 0 \\ 0 & 0 & 0 & 0 & 2 \\ 0 & 0 & 0 & 0 & 0 \end{pmatrix}, \quad S_- = \begin{pmatrix} 0 & 0 & 0 & 0 & 0 \\ 2 & 0 & 0 & 0 & 0 \\ 0 & \sqrt{6} & 0 & 0 & 0 \\ 0 & 0 & \sqrt{6} & 0 & 0 \\ 0 & 0 & 0 & 2 & 0 \end{pmatrix}. \tag{3.19}$$

The exact results for the spin system from Eq. (3.17) can be seen in Fig. 3.6.

3.3.2 Stochastic differential equations

For a collective spin system the total number of excitations $a^\dagger a + b^\dagger b$ stays conserved. Thus, S can be defined as

$$S = \frac{1}{2}(a^\dagger a + b^\dagger b) \tag{3.20}$$

and

$$\langle S \rangle = \frac{1}{2}\big(\langle a^\dagger a \rangle + \langle b^\dagger b \rangle \big), \tag{3.21}$$

which can be used to fix the initial condition for α and β. For the stochastic calculations we set α as fully occupied and β in the ground state:

$$|\Psi(t=0)\rangle = |\alpha = \sqrt{2S}\rangle \otimes |\beta = 0\rangle = |\sqrt{2S}, 0\rangle\,. \tag{3.22}$$

The stochastically calculated trajectories

$$d\alpha(t) = -\frac{\Gamma}{2}\left(|\beta|^2 + \frac{(1+k)}{2}\right)\alpha dt + \sqrt{\frac{\Gamma(1-k)}{4}\left(|\beta|^2 + \frac{1+k}{2}\right)}dW, \tag{3.23}$$

$$d\beta(t) = \frac{\Gamma}{2}\left(|\alpha|^2 - \frac{(1-k)}{2}\right)\beta dt + \sqrt{\frac{\Gamma(1+k)}{4}\left(|\alpha|^2 - \frac{1-k}{2}\right)}dW \tag{3.24}$$

can then be averaged to evaluate the expectation values we are interested in, like

$$\langle S_z \rangle = \frac{1}{2}\big(\langle a^\dagger a \rangle - \langle b^\dagger b \rangle \big). \tag{3.25}$$

Here the two SDEs have to run simultaneously as they depend on each other.

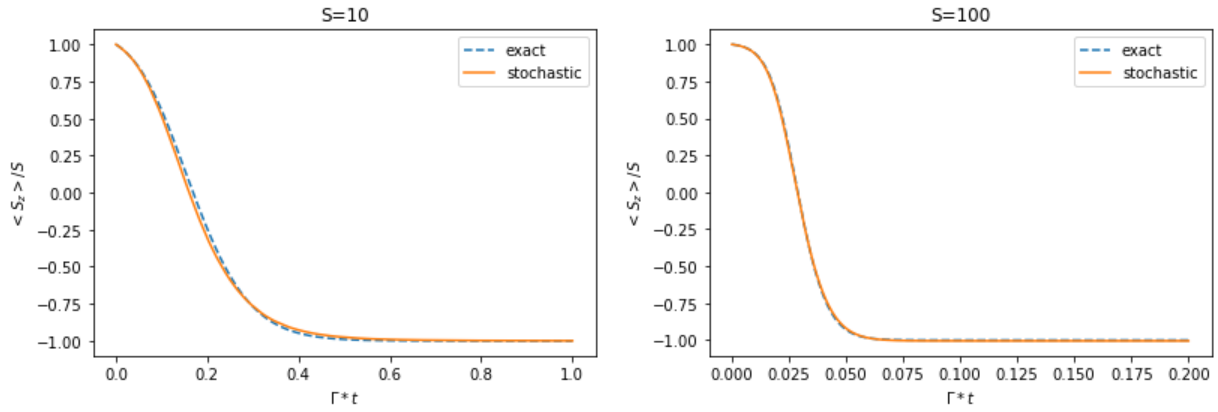

Figure 3.6: $\langle S_z \rangle (t)/S$ exact and stochastic using the P-function; $n_{traj} = 5000$ for the stochastic plot lines; the plots (especially for $S = 100$) show the phenomenon of superradiance [4], which occurs in collective spin systems.

3.4 Spin system coupled to a harmonic oscillator

Simulating the master equation

$$\frac{d\rho}{dt} = -i[H,\rho] + \frac{\Gamma}{2S}\mathcal{D}[S_-]\rho + \kappa\mathcal{D}[c]\rho \tag{3.26}$$

with the Euler method [2] is no longer reasonable in terms of computing power as the whole Hilbert space is now given by $\mathcal{H} = \mathcal{H}_S \otimes \mathcal{H}_{HO}$, which means multiplying the dimensions of the spin system and the harmonic oscillator.

3.4.1 Stochastic differential equations

The SDEs from section 2.7.3,

$$d\alpha(t) = -\left[\frac{\Gamma}{2S}\left(|\beta|^2 + \frac{(1+k)}{2}\right)\alpha + i\frac{g}{\sqrt{2S}}\beta\gamma\right]dt + \sqrt{\frac{\Gamma(1-k)}{4S}\left(|\beta|^2 + \frac{1+k}{2}\right)}dW, \tag{3.27}$$

$$d\beta(t) = \left[\frac{\Gamma}{2S}\left(|\alpha|^2 - \frac{(1-k)}{2}\right)\beta - i\frac{g}{\sqrt{2S}}\alpha\gamma^*\right]dt + \sqrt{\frac{\Gamma(1+k)}{4S}\left(|\alpha|^2 - \frac{1-k}{2}\right)}dW, \tag{3.28}$$

$$d\gamma(t) = -\left(\kappa\gamma + i\frac{g}{\sqrt{2S}}\alpha\beta^*\right)dt + \sqrt{\frac{\kappa(1-k)}{2}}dW, \tag{3.29}$$

were also simulated with the Euler-Maruyama method [2]. If we set $\kappa = \Gamma = 0$, $g = 1$ only the coupling term remains in the equations causing the system to oscillate between the spin and the cavity. Normally $\langle S_z \rangle$ would oscillate endlessly from highest excited state to ground state. But while oscillating the system 'loses' information due to the stochastic nature of the calculation. The oscillation gets weaker as κ gets closer to 1 (Fig. 3.7) and vanishes completely for $\kappa \geq 1$ (Fig. 3.8).

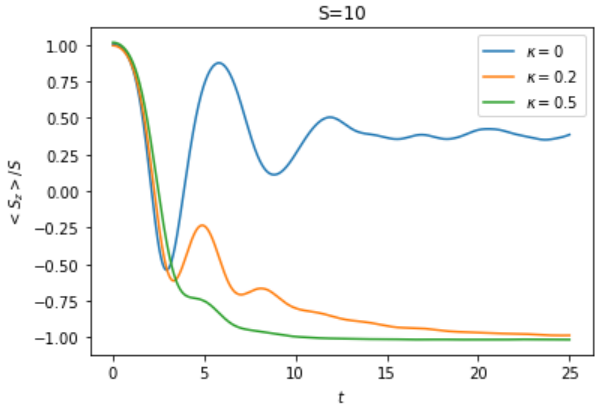

Figure 3.7: $\langle S_z \rangle (t)/S$ for $g = 1$, $\Gamma = 0$ and $\kappa = \{0, 0.2, 0.5\}$ with the Wigner function; $n_{traj} = 2000$

The two cases considered in Section 2.7.1, $g = 1, \kappa > g, \Gamma = 0$ and $g = \kappa = 0, \Gamma \neq 0$, can now be compared on the basis of the program for $\Gamma = g^2/\kappa$. In Fig. 3.8 and Fig 3.9 one can see that the approximation $\langle \dot{c} \rangle \approx 0$ gets more accurate for large ratios of κ/g.

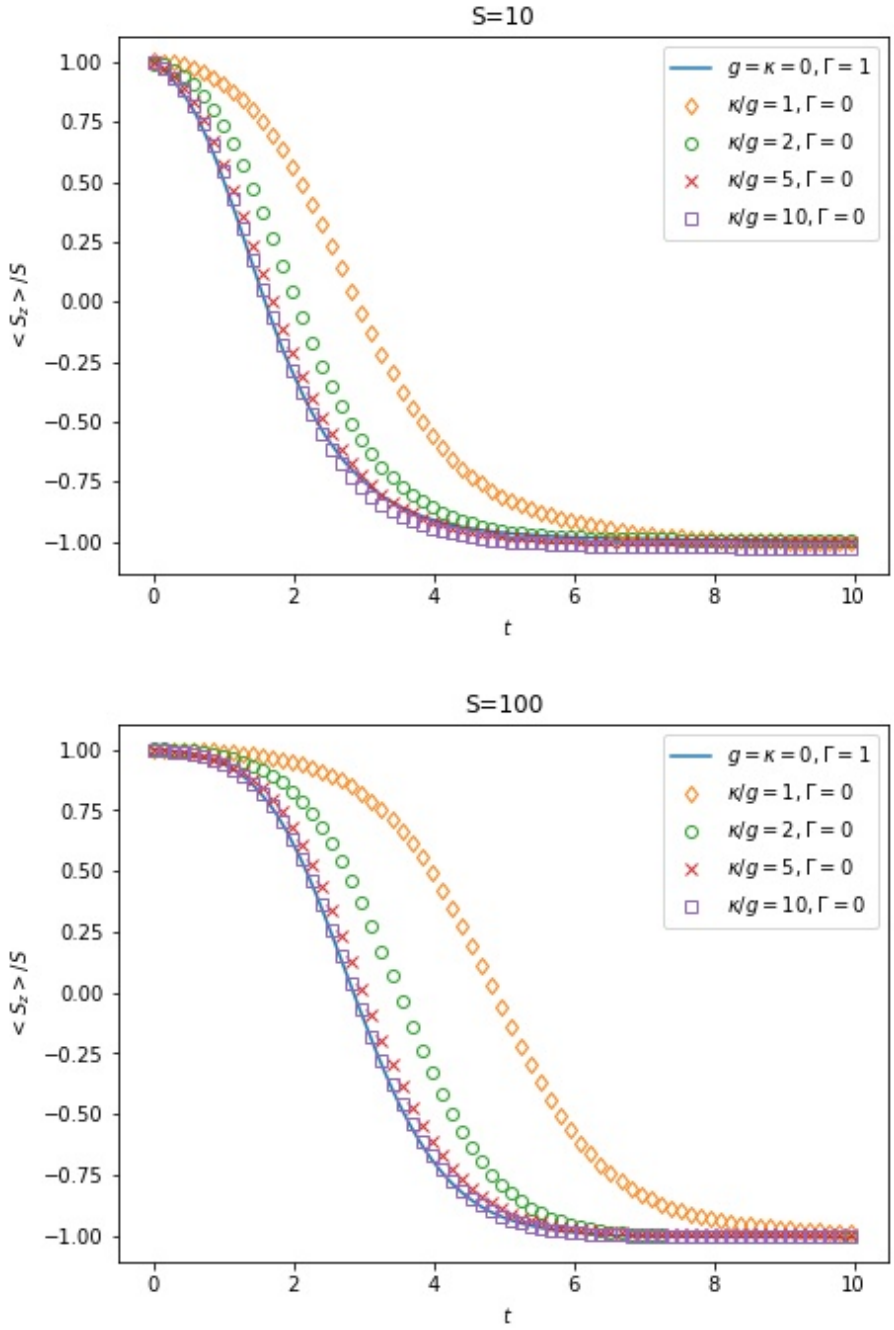

Figure 3.8: $\langle S_z \rangle (t)/S$ with $S = 10$ and $S = 100$; for each of the two cases: $g = \kappa = 0$, $\Gamma = 1$ and $\kappa/g = \{1, 2, 5, 10\}$, $\Gamma = 0$ using the Wigner function for $n_{traj} = 2500$

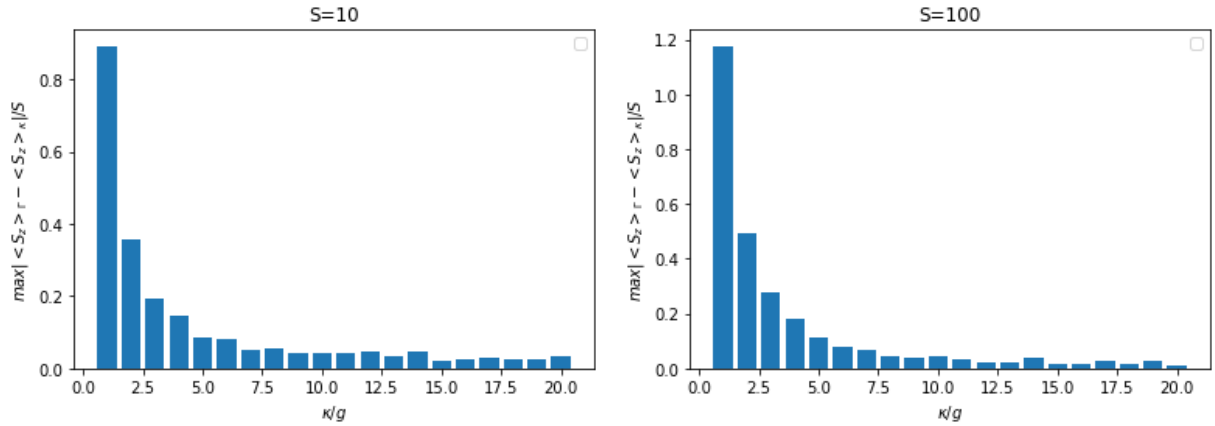

Figure 3.9: Maximal difference between the values of $\langle S_z \rangle / S$ obtained from the stochastic simulations for $g = \kappa = 0$, $\Gamma = 1$ ($\langle S_z \rangle_\Gamma$) and for $\Gamma = 0$, $\kappa/g = [1; 20]$ ($\langle S_z \rangle_\kappa$) for each $S = 10$ and $S = 100$ using the Wigner function; $n_{traj} = 2500$; the graphs show a strong exponential decrease for small κ/g while slowing down to a almost constant difference for a growing κ/g and ultimately to zero. The difference corresponds to the accuracy of the simulation respectively of the approximation $\langle \dot{c} \rangle \approx 0$.

4 Conclusion

In the theoretical part - chapter 2 - the master equation formalism of the Dicke model [9] is introduced. Through phase space distributions [9] the master equations are translated into Fokker-Planck equations [9] and by arranging their coefficients into matrix form they are mapped onto SDEs [2] using the truncated Wigner approximation [6] and the positive diffusion approximation [5]. This laborious conversion pays off in form of an efficiency enhancement for the simulation of the featured systems in the numerical part - chapter 3.

In case of the quantum harmonic oscillator, the exact (numerical) solutions for the expectation values get accurate for a sufficient amount of considered states which is $\sim 10N_{th}$. But the more states are considered the less efficient the simulation gets as the matrices used for calculation are $n \times n \times n_t$ matrices (n_t ... amount of time steps). A more effective performance is delivered by the stochastic approach. Here the dimension of the operating matrix is (more or less - depending on the approach of the program) reduced to $n_t \times n_{traj}$ which is in general independent of the dimension of the system itself. Also a value of about $n_{traj} = 1000$ trajectories was (or would have been) adequate for each of the simulations executed in the course of this thesis. This means that, in case of spin systems, expectation values of relatively large ensembles of N two-level systems can still be calculated stochastically while they are impossible to solve analytically or by an exact numerical approach ($d_{\mathcal{H}} = 2S+1 = N+1$).

Efficiency can further be enhanced in the case of collective spin systems coupled to a quantum harmonic oscillator. In the master equation the term for the spin system can be neglected by setting its dissipation coefficient $\Gamma = 0$, leaving the term responsible for the coupling with the coupling strength g and the term for the harmonic oscillator with the damping coefficient κ. We find that for $\kappa \gg g$ the approximation $\langle \dot{c} \rangle \approx 0$ can be performed. This leads to a specific form of the dynamics of the various expectation values (Eq. (2.79) to (2.82)) which is identical to the expectation values of the uncoupled spin system ($g = \kappa = 0, \Gamma \neq 0$) except for the pre-factors. By a subsequent comparison of these factors one finds that both systems - the coupled oscillator and the spin system itself - can be described by each other separately for $\Gamma = g^2/\kappa$. This is verified by the simulation in Fig. 3.8. As stated above this works well for rather large values of κ/g, which can be seen in Fig. 3.9. Mathematically the expression of a quantum harmonic oscillator has a more simple form compared to an arbitrary spin system. A relatively complex spin system can therefore be simulated approximately by a 'simple' quantum harmonic oscillator.

A Appendix

The following code corresponds to the plot used to produce Fig. 3.6 (P-function):

```
import numpy as np
import matplotlib.pyplot as plt
import matplotlib

def dW(step): #Wiener increment
    sqrtdt=np.sqrt(step)
    dW_real=np.random.normal(0.0,sqrtdt,size=(1,m))
    dW_imaginary=1j*np.random.normal(0.0,sqrtdt,size=(1,m))
    return (dW_real+dW_imaginary)

def maruyama_P(t,step,dW):
    sqrtdt=np.sqrt(step)
    alpha=np.ones((len(t),m),dtype=complex)*np.sqrt(s*2) #initial condition
    beta=np.ones((len(t),m),dtype=complex)*np.sqrt(s)*0

    for i in range(0,len(t)-1):
        A=-gamma/2*(np.abs(beta[i])**2+(1+k)/2)*alpha[i] #alpha
        B=np.sqrt(gamma*((1-k)/4)*(np.abs(beta[i])**2+(1+k)/2)) #alpha

        C=gamma/2*(np.abs(alpha[i])**2-(1-k)/2)*beta[i] #beta
        D=np.sqrt(gamma*((1+k)/4)*(np.abs(alpha[i])**2-(1-k)/2)) #beta

        alpha[i+1]=alpha[i]+A*step+B*dW(step)
        beta[i+1]=beta[i]+C*step+D*dW(step)
    return alpha,beta

def mean(t,y,m):
    y_mean1=np.zeros(len(t),dtype=complex) #mean of alpha
    y_mean2=np.zeros(len(t)) #mean of |alpha|^2
    for i in range(1,m):
        y_mean1=y_mean1+y[:len(t),i-1]
        y_mean2=y_mean2+np.abs(y[:len(t),i-1])**2
    return y_mean1,y_mean2

def P(t,y,m): #averaging over the trajectories
    y_mean1,y_mean2=mean(t,y,m)
    y_mean1=y_mean1/m
    y_mean2=y_mean2/m
    return y_mean1,y_mean2

m=500 #amount of trajectories

```

```
#parameters
s=10
N_th=5
gamma=1
step=0.001 #time stepwidth
t_end=1

k=1 #P(k=1), Q(k=-1), Wigner(k=0)

t=np.linspace(0,t_end,int(t_end/step))

alpha,beta=maruyama_P(t,step,dW)
alpha_mean1,alpha_mean2=P(t,alpha,m)
beta_mean1,beta_mean2=P(t,beta,m)

Sz_mean=0.5*(alpha_mean2-beta_mean2)

plt.plot(t,Sz_mean/s)

plt.xlabel(r"$t$")
plt.ylabel(r"$<S_z>/S$")
```

Bibliography

[1] R. H. Dicke. *Coherence in spontaneous radiation processes*, Phys. Rev. **93**, 99 (1954).

[2] Crispin Gardiner. *Stochastic methods*. Springer, 2009.

[3] Roy J Glauber. *Coherent and incoherent states of the radiation field*. Phys. Rev. **131**, 2766 (1963).

[4] M. Gross and S. Haroche. *Superradiance: An Essay on the Theory of Collective Spontaneous Emission*, Phys. Rep. **93**, 301 (1982).

[5] Julian Huber, Peter Kirton and Peter Rabl. *Phase-Space Methods for Simulating the Dissipative Many-Body Dynamics of Collective Spin Systems*. SciPost Phys. **10**, 045 (2021).

[6] Anatoli Polkovnikov. *Phase space representation of quantum dynamics*. Annals of Physics **325**, 1790 (2010).

[7] Franz Schwabl. *Quantenmechanik (QM I): Eine Einführung*. Springer, 2007.

[8] Julian Schwinger. *On angular momentum*. Technical Report, U.S. Atomic Energy Commission, Web. doi:10.2172/4389568, 1952.

[9] Daniel F. Walls and Gerard J. Milburn. *Quantum Optics*. Springer, 2008.